



HAL
open science

Bidirectional real-time hybrid test on a steel column virtually connected to a reinforced concrete substructure

Bastien Bodnar, Magdalini Titirla, Fabrice Gatuingt, Frédéric Ragueneau

► **To cite this version:**

Bastien Bodnar, Magdalini Titirla, Fabrice Gatuingt, Frédéric Ragueneau. Bidirectional real-time hybrid test on a steel column virtually connected to a reinforced concrete substructure. EURODDYN 2023 - XII International Conference on Structural Dynamics, Jul 2023, Delft, Netherlands. hal-04303424

HAL Id: hal-04303424

<https://hal.science/hal-04303424>

Submitted on 23 Nov 2023

HAL is a multi-disciplinary open access archive for the deposit and dissemination of scientific research documents, whether they are published or not. The documents may come from teaching and research institutions in France or abroad, or from public or private research centers.

L'archive ouverte pluridisciplinaire **HAL**, est destinée au dépôt et à la diffusion de documents scientifiques de niveau recherche, publiés ou non, émanant des établissements d'enseignement et de recherche français ou étrangers, des laboratoires publics ou privés.

BIDIRECTIONAL REAL-TIME HYBRID TEST ON A STEEL COLUMN VIRTUALLY CONNECTED TO A REINFORCED CONCRETE SUBSTRUCTURE

B. Bodnar^{1,2}, M. Titirla¹, F. Gatuingt², and F. Ragueneau^{2,3}

¹ Conservatoire National des Arts et Métiers, Laboratoire de Mécanique des Structures et des Systèmes Couplés, 292 rue Saint-Martin, 75141 Paris cedex 03, France

² Université Paris-Saclay, Centrale Supélec, ENS Paris-Saclay, CNRS, Laboratoire de Mécanique Paris-Saclay, 91190, Gif-sur-Yvette, France

³ EPF École d'Ingénieurs, 55 av. Président Wilson, F-94230, Cachan, France

bastien.bodnar@lecnam.net; magdalini.titirla@lecnam.net;
fabrice.gatuingt@ens-paris-saclay.fr; frederic.ragueneau@ens-paris-saclay.fr;

Abstract. This paper presents the results of a bidirectional Hardware-in-the-Loop (HiL) real-time hybrid test on a steel column connected to a two-story reinforced concrete (RC) substructure under earthquake conditions. Two hydraulic dynamic actuators apply the horizontal displacements at the top of the specimen. Nonlinear multi-fiber beam elements model the numerical substructure. The computational cost of the finite element (FEM) analysis is reduced using a Proper Orthogonal Decomposition (POD) Unassembled Discrete Empirical Interpolation Method (UDEIM) with a non-iterative α -Operator Splitting (α -OS) time integration scheme. Data acquisition is carried out using a Linux[®] real-time (RT) target, while the dynamic analysis is performed on a Windows[®] host computer running custom procedures implemented in MATLAB[®] software. A LABVIEW[®] interface connects both systems via a lossless stream network. Results on the present case study show that: (1) using a hyper-reduced order model (HROM) can accelerate costly nonlinear dynamic analyses so that they can be run above the sampling period of the ground motion during hybrid tests, and (2) using lossless stream networks calling a MATLAB[®] kernel efficiently combines the high data acquisition speed of RT targets (i.e., 10 μ s per sample) with the computing power of host computers since the data exchange is quasi-instantaneous.

1. Introduction

Tests on sensitive structural elements (e.g., columns, beams, or frames) are sometimes necessary to study the behavior of civil engineering structures (e.g., dynamic response, damage, or failure mechanisms) under earthquake conditions. Quasi-static “push-over” or dynamic tests are carried out for this purpose. However, these approaches are limited since it is not possible to experimentally consider the inertial forces during “push-over” tests, while the similitude theory leads to the addition of masses on the reduced specimens during dynamic experiments on shaking tables or in centrifuge facilities. As a result, unrealistic collapse mechanisms may appear.

To overcome these limitations, “hybrid tests” have been developed over the last decades. They allow for the assessment of the dynamic response of specimens at full scale considering numerically the

environment in which they are installed. The commands of the actuators loading the specimen are computed through a dynamic analysis carried out simultaneously on a numerical model including all the untested components.

A common approach, called Pseudo-Dynamic (PsD), consist of applying the displacements in deferred time [1]. Such experiments are easier to perform than Real-Time (RT) hybrid tests since the real time can only be reached provided that the delay of the overall process (including the FEM analysis, the movement of the actuators, the measurements, and the data exchange) is lower than the sampling period of the ground motion (i.e., approximately equal to 10 ms). This can be difficult to achieve since nonlinear material laws are required to accurately consider the decrease of stiffness due to damage during earthquakes. To avoid iterating and prevent the risk of overshoot (i.e., sudden collapse of the specimen), an Operator Splitting (OS) method was developed [2]. The restoring force vector is split into a nonlinear term based on an explicit prediction of the displacements and a linear term depending on the elastic stiffness matrix. This integration scheme, called α -OS, was successfully applied to perform PsD hybrid tests using in-plane numerical substructures made of linear elements [3], elastic-plastic hinges [4], or multifibre beam elements ([5], [6]), while only linear elements or nonlinear macro elements were used in real time [7]. To the best of our knowledge, the use of semi-global approaches (e.g., multifibre beam elements, or multilayer shell elements) to carry out RT hybrid tests using out-of-plane models has not been investigated yet due to their computational cost, even if recent advances in Reduced Order Modelling (ROM) could advantageously be used to decrease the delay of Hardware-in-the-Loop (HIL) procedures involving high dimensional nonlinear systems. *A posteriori* methods are useful here since the properties of the external loading, the tested specimen, and the numerical substructure are all known so that accurate snapshots can be pre-compute. A modal basis can be built using a Proper Orthogonal Decomposition (POD) method [8]. In addition, the computational cost due to the assessment of the nonlinear terms of the matrix system can be reduced using hyper reduction procedures such as the Unassembled Discrete Empirical Interpolation Method (UDEIM) [9]. The UDEIM consists of approximating the nonlinear terms based on samples assessed on a set of elements belonging to a Reduced Integration Domain (RID). Such a method drastically reduces the computational cost of FEM analyses since only a small number of elements needs to be update during the online phase, making Hyper Reduced Order Models (HROMs) useful to decrease the delay of hybrid tests procedures.

Efficient measurement devices guaranteeing a quasi-instantaneous data acquisition also need to be used to successfully perform RT hybrid tests. Embedded Linux[®] RT targets meet this requirement since they are able to measure and read data on demand with a delay approximately equal 10 μ s. A host computer and a lossless exchange network ensuring high speed data transfers with the RT target (e.g., stream network) are also required to simultaneously run the FEM analysis in real time.

This paper presents the results of a bi-directional HiL real-time hybrid test on a steel column virtually connected at its top to a two-story RC structure under earthquake conditions. The study emphasizes on efficiently integrating the finite element solver in the testing procedure, reducing the computational cost of the simulated substructure, and ensuring quasi-instantaneous data exchange between the components of the experimental set-up. In Section 2, the non-iterative α -OS time scheme and the substructuring method are detailed. The Section 3 summarizes the POD-UDEIM hyper reduction procedure. The case study, the experimental set up, and its components (e.g., host computer, Linux[®] RT target, and actuators) are described in Section 4. The Section 5 presents the HROM (i.e., number of modes, time-savings), a benchmark comparison of the methods available in LabVIEW[®] for running FEM analyses, and experimental results (e.g., delays, or comparison between the commands and the displacements).

2. Times integration scheme and substructuring method

The α -OS time integration scheme is based on the classical Hilber-Huges-Taylor (HHT) method [10] and consists of splitting the restoring force vector into a nonlinear part $\tilde{\mathbf{r}}^{\text{NL}}(\tilde{\mathbf{u}})$ approximated using an explicit prediction of the displacements, and a linear part depending on the elastic stiffness matrix (1):

$$\mathbf{r}(\mathbf{u}) \cong \mathbf{K}_E \cdot \mathbf{u} + \tilde{\mathbf{r}}^{\text{NL}}(\tilde{\mathbf{u}}) \quad \text{with} \quad \tilde{\mathbf{r}}^{\text{NL}}(\tilde{\mathbf{u}}) = \tilde{\mathbf{r}}(\tilde{\mathbf{u}}) - \mathbf{K}_E \cdot \tilde{\mathbf{u}} \quad (1)$$

where \mathbf{K}_E is the elastic stiffness matrix, \mathbf{u} is the displacement vector, $\tilde{\mathbf{u}}$ is the explicit prediction of the displacement vector, and $\tilde{\mathbf{r}}(\tilde{\mathbf{u}})$ is the prediction of the restoring force vector. The system of linear equations to be solved to compute $\ddot{\mathbf{u}}_{n+1}$ at time step $n + 1$ is thus given in (2) by introducing (1) into the equation of motion:

$$\widehat{\mathbf{M}} \cdot \ddot{\mathbf{u}}_{n+1} = \widehat{\mathbf{F}}_{n+1+\alpha} \quad (2)$$

where $\widehat{\mathbf{M}}$ is the pseudo mass matrix, and $\widehat{\mathbf{F}}_{n+1+\alpha}$ is the pseudo force vector [11]. One can note that the method depends on an α parameter usually set between $-1/3$ and 0 . However, a value close to -0.05 is recommended [10]. During hybrid tests, the high frequency content due to the measurement noise is thus dampened. The α -OS method is implicit in the linear phase and explicit in the nonlinear phase. As demonstrated in practical cases, the residual error due to the approximation in (1) is almost negligible in the case of dynamic FEM analyses on RC structures subjected to infinitesimal strains [12]. The numerical substructure and the tested specimen are then split to introduce the restoring forces applied by the actuators as external loads on the common DOFs, as shown in the example in Figure 1.

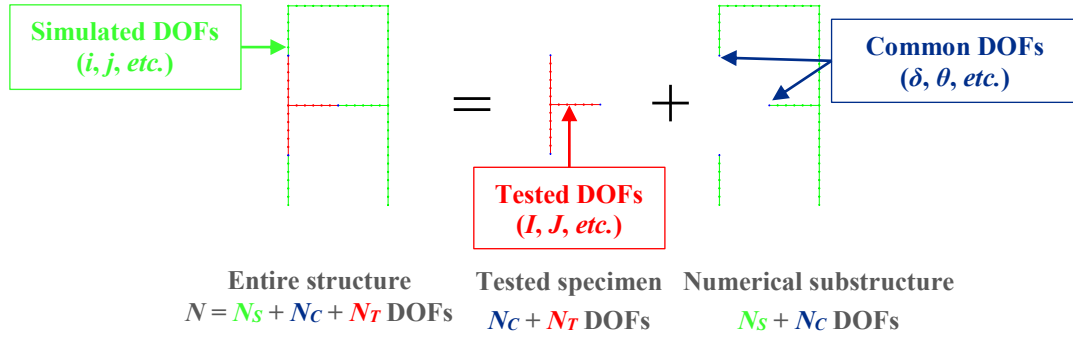


Figure 1: Substructuring of an in-plane two-storey frame.

Among the N DOFs, N_S DOFs only belong to the modelled substructure (subscript I and j), N_C belong to both the modelled substructure and the tested specimen (subscript δ and θ), and N_T only belong to the tested specimen (subscript I and J). By distinguishing in (2) the systems of equations coming from the numerical substructure (subscripted S), and the tested specimen (subscripted T), it is possible to reorganize the matrix $\widehat{\mathbf{M}}$ and the related terms as described in (3):

$$\begin{bmatrix} {}^S\widehat{\mathbf{M}}_{ij} & {}^S\widehat{\mathbf{M}}_{i\theta} & \mathbf{0} \\ {}^S\widehat{\mathbf{M}}_{\delta j} & {}^S\widehat{\mathbf{M}}_{\delta\theta} + {}^T\widehat{\mathbf{M}}_{\delta\theta} & {}^T\widehat{\mathbf{M}}_{\delta J} \\ \mathbf{0} & {}^T\widehat{\mathbf{M}}_{I\theta} & {}^T\widehat{\mathbf{M}}_{IJ} \end{bmatrix} \cdot \begin{bmatrix} \ddot{\mathbf{u}}_{j,n+1} \\ \ddot{\mathbf{u}}_{\theta,n+1} \\ \ddot{\mathbf{u}}_{J,n+1} \end{bmatrix} = \begin{bmatrix} {}^S\widehat{\mathbf{F}}_{i,n+1+\alpha} \\ {}^S\widehat{\mathbf{F}}_{\delta,n+1+\alpha} + {}^T\widehat{\mathbf{F}}_{\delta,n+1+\alpha} \\ {}^T\widehat{\mathbf{F}}_{I,n+1+\alpha} \end{bmatrix} \quad (3)$$

where $\ddot{\mathbf{u}}_{j,n+1}$, $\ddot{\mathbf{u}}_{\theta,n+1}$ and $\ddot{\mathbf{u}}_{J,n+1}$ are the acceleration vectors related to the simulated, common, and tested DOFs, respectively. The measured restoring force vector ${}^T\tilde{\mathbf{r}}_{\delta,n+1}$ is introduced in the pseudo force vector ${}^T\widehat{\mathbf{F}}_{\delta,n+1+\alpha}$, whereas the restoring force vectors computed on the numerical substructure ${}^S\tilde{\mathbf{r}}_{i,n+1}$ and ${}^S\tilde{\mathbf{r}}_{\delta,n+1}$ are introduced in ${}^S\widehat{\mathbf{F}}_{i,n+1+\alpha}$ and ${}^S\widehat{\mathbf{F}}_{\delta,n+1+\alpha}$, respectively [11].

At the time step $n + 1$, the matrix system in (3) is first reduced by condensing the components of $\ddot{\mathbf{u}}_{j,n+1}$ so that the entries of the acceleration vector can be computed on the common DOFs. Once $\ddot{\mathbf{u}}_{\theta,n+1}$ is known, the entries related to the simulated DOFs (stored in $\ddot{\mathbf{u}}_{j,n+1}$) are then assessed by solving the equations indexed i in (3).

3. Reduced order modelling using a POD-UDEIM approach

This paper proposes to reduce the computational cost of the simulated substructure using a POD method combined with a UDEIM approach. Nonlinear FEM analyses are first performed on a Full Order Model

(FOM) including both the numerical and the tested components. Displacement snapshots are then used as training data to compute nonlinear POD modes by carrying out a Singular Value Decomposition (SVD) on the simulated DOFs. The n first POD modes are then selected to build a reduced modal basis. This a posteriori approach reduces the number of DOFs as well as the computational cost of the matrix operations. The displacement vector related to the simulated substructure ${}^S\mathbf{u} \in \mathbb{R}^{N_s+N_c}$ can thus be expressed according to a new POD basis $\Phi \in \mathbb{R}^{N_s \times n}$, as described in (4):

$${}^S\mathbf{u} = \begin{pmatrix} \mathbf{u}_j \\ \mathbf{u}_\theta \end{pmatrix} \approx \Gamma \cdot {}^S\mathbf{q} \quad \text{with} \quad \Gamma = \begin{bmatrix} \Phi & \mathbf{0} \\ \mathbf{0} & I_d \end{bmatrix}, \quad {}^S\mathbf{q} = \begin{pmatrix} \mathbf{q}_j \\ \mathbf{u}_\theta \end{pmatrix}, \quad \text{and} \quad \Phi = [\varphi_1 \quad \dots \quad \varphi_n] \quad (4)$$

where $\mathbf{q}_j \in \mathbb{R}^n$ is the displacement vector related to the N_s simulated DOFs in the reduced basis Φ , $\varphi_{i=1,\dots,n} \in \mathbb{R}^{N_s}$ is the i^{th} POD mode computed using a SVD procedure, and $I_d \in \mathbb{R}^{N_c \times N_c}$ is an identity matrix.

In addition, a UDEIM interpolation operator is here added to the solving process. To do so, a second SVD is performed on the force snapshots related to the nonlinear parts of the unassembled restoring force vector (i.e., computed element per element) (5):

$${}^S\tilde{\mathbf{r}}^{\text{NL,u}}({}^S\mathbf{u}) = {}^S\tilde{\mathbf{r}}^{\text{u}}({}^S\mathbf{u}) - \mathbf{K}_E^{\text{u}} \cdot \mathbf{B} \cdot \begin{pmatrix} \tilde{\mathbf{u}}_j \\ \tilde{\mathbf{u}}_\theta \end{pmatrix} \quad (5)$$

where N_e is the number of simulated finite elements, N_f is the number of force entries per element, $\mathbf{K}_E^{\text{u}} \in \mathbb{R}^{N_e \cdot N_f \times N_e \cdot N_f}$ is the unassembled elastic stiffness matrix of the simulated substructure, $\mathbf{B} = [\mathbf{L}_1^T \quad \dots \quad \mathbf{L}_{N_e}^T]^T \in \mathbb{R}^{N_e \cdot N_f \times (N_s+N_c)}$ is a Boolean assembly matrix, $\mathbf{L}_{e=1,\dots,N_e} \in \mathbb{R}^{N_f \times (N_s+N_c)}$ is a collocation matrix used to select the displacements of the nodes connected to the e^{th} finite element, and $\tilde{\mathbf{u}}_j$ and $\tilde{\mathbf{u}}_\theta$ are the explicit predictions of the displacement on the simulated and common DOFs, respectively.

The m first force modes are then selected to build a second truncated modal basis $\Psi = [\psi_1 \quad \dots \quad \psi_m] \in \mathbb{R}^{N_e \cdot N_f \times m}$. A DEIM algorithm is next to find for each UDEIM mode $\psi_i \in \mathbb{R}^{N_e \cdot N_f}$ the best collocation entries [15]. The material laws are updated on the elements belonging to the RID (i.e., where the nonlinear part of the unassembled restoring force vector needs to be computed). The k collocation entries belonging to the RID are then used as samples to build an explicit prediction of the reduced restoring force vector ${}^S\tilde{\mathbf{r}} \in \mathbb{R}^{n+N_c}$, as described in (6):

$${}^S\tilde{\mathbf{r}}(\Gamma \cdot {}^S\tilde{\mathbf{q}}) = \Gamma^T \cdot \mathbf{B}^T \cdot \left((\mathbf{I}_d - \mathbf{A} \cdot \mathbf{P}^T) \cdot \mathbf{K}_E^{\text{u}} \cdot \mathbf{B} \cdot \Gamma \cdot {}^S\tilde{\mathbf{q}} + \mathbf{A} \cdot {}^S\tilde{\mathbf{r}}_{\text{RID}}^{\text{u}}(\Gamma \cdot {}^S\tilde{\mathbf{q}}) \right) \quad (6)$$

with $\mathbf{A} = \Psi \cdot (\mathbf{P}^T \cdot \Psi)^+$

where $\mathbf{P} \in \mathbb{R}^{N_e \cdot N_f \times k}$ is a Boolean partition matrix that refers the k collocation entries, $\Gamma \in \mathbb{R}^{(n+N_c) \times (N_s+N_c)}$ is the reduced basis related to the numerical substructure, ${}^S\tilde{\mathbf{q}} \in \mathbb{R}^{n+N_c}$ is the approximation of the displacement vector in basis Γ , and $\mathbf{A} \in \mathbb{R}^{N_e \cdot N_f \times k}$ is the UDEIM interpolation operator. Thus, the CPU time related to the simulated substructure can be considerably reduced since only the internal variables of the elements belonging to the RID need to be updated.

4. Case study and experimental set-up

4.1. Case study

The case study consisted of a tested steel column virtually connected to the southeast corner of a two-story RC building (see Figure 2 (a)) loaded by the ground motion in Figure 2 (b). The specimen was embedded to a reaction wall via an end plate, and was loaded at its top by two dynamic actuators modeling a bidirectional pin connection along the x and y -axes. The vertical displacement and force entries (i.e., along the z -axis) were computed numerically to simplify the experimental set-up.

A 3 m long HEA 200 steel column was taken as a tested specimen. Elastic stiffnesses $K_{xx} = 545 \times 10^3$ N/m, $K_{yy} = 169 \times 10^3$ N/m, and $K_{zz} = 377 \times 10^6$ N/m modeled its action on the common

DOFs (subscript δ and θ) using the pseudo mass matrix ${}^T \widehat{\mathbf{M}}_{\delta\theta}$ (3). K_{xx} and K_{yy} were directly measured on the experimental set-up, and no tested DOF (subscript I and J) was taken into account since the steel column was embedded to the ground level.

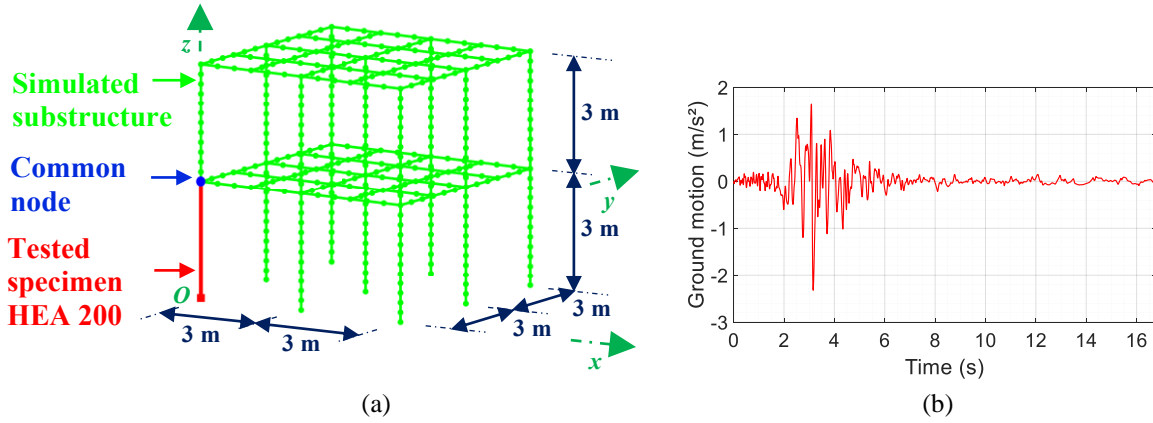


Figure 2: Mesh of the building (a), and ground acceleration versus time (b).

The numerical substructure was modeled by 405 nodes linked by 444 multifibre beam elements [13]. All the columns were embedded to the floor level, and 2382 free DOFs modeled the building. The stories were 3 m high, and each span was 3 m long (see Figure 2 (a)). A mass per unit area of 500 kg/m² was applied to both floors *via* the transversal and longitudinal beams. The columns had a 15 × 15 cm square cross-section, and the beams had a 15 × 25 cm rectangular one. The diameter of each longitudinal steel rebar was set at 12 mm, and the steel coating was 20 mm (see Figure 3 (a)). The cross-sections of the beams and the columns were divided into 3 × 5 and 3 × 3 surface elements, respectively. The concrete fibers were located at the integration points of the surface elements (grey dots), while the steel fibers (blue dots) were located at 34 mm from the corners of the cross-sections (see Figure 3 (b)).

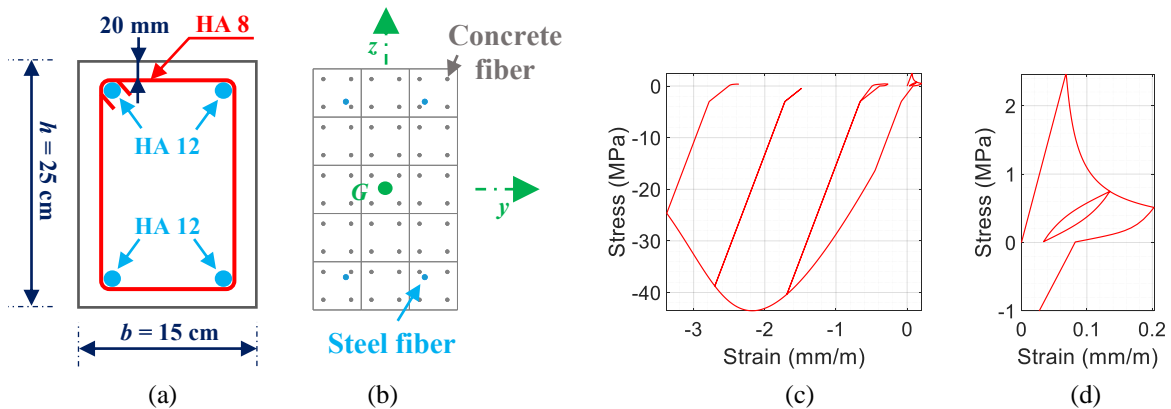


Figure 3: Mesh of a simply supported beam with two multifibre beam elements (a), and cross-section of the beams: steel reinforcements (b), and mesh (c).

Knowing that the length/height ratio of the structural components (e.g., beams, or columns) is usually higher than 10 in civil engineering structures, the damage was assumed to be mainly due to bending. A “unilateral” damage law with frictional sliding developed to model quasi-brittle materials under dynamic or cyclic loadings [14] was used for concrete fibers (see Figure 3 (c) & (d)), while a bilinear elastic-plastic law modeled the steel rebars, with an elastic modulus of 210 GPa, a yielding stress of 500 MPa, and a kinematic hardening of 1 GPa. A Rayleigh viscous damping ratio modeled the structural damping due to the viscosity of air and materials, or discontinuities at junctions. It was set at $\zeta = 2\%$ at $f_1 = 1.47$ Hz (eigenfrequency #1) and $f_6 = 5.50$ Hz (eigenfrequency #6) so that its value reached a

minimum around the main eigenmodes. Factors equal to 1.10 in the x-direction, 0.50 in the y-direction, and 0.30 in the z-direction weighed the ground motion in Figure 2 (b), while the dead and live loads were statically applied before entering the time step loop.

4.2. Experimental set-up

The experiment was performed on the RESIST testing platform of the LMPS laboratory (see Figure 4 (a)). The HEA 200 steel column was set up horizontally, and embedded to a reaction wall *via* an end plate. Two horizontal and vertical dynamic actuators equipped with accumulators and pin connected to a frame structure loaded the steel column along the *x* and *y*-axes, respectively. Both had a maximum capacity of 250 kN, a stroke of ± 125 mm, and an oil flow up to 280 L/min.

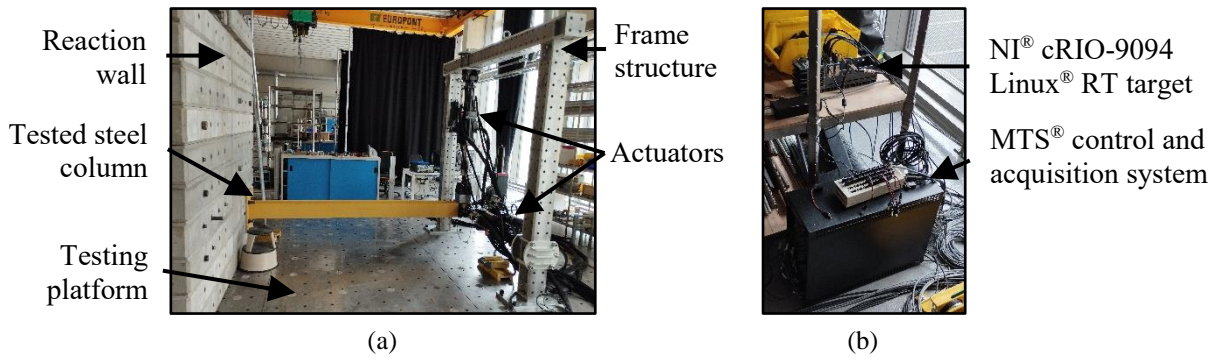


Figure 4: Experimental set-up (a) and focus on the MTS[®] system and the Linux[®] RT target.

The Proportional Integrative Derivative (PID) controller was managed by a MTS[®] system dealing with analog data. Simultaneously, an Intel[®] Core™ i7-12800H CPU @ 3.40 GHz and 32 GB RAM Windows[®] host computer dealing with numerical data ran the nonlinear dynamic analysis on the simulated substructure. Both systems were connected by a National Instrument[®] CompactRIO 9049 Linux[®] RT target (see Figure 4 (b)) writing, reading, and converting data quasi-instantaneously (i.e., in approximately 10 μ s per time step). The RT target converted the commands of the actuators from numeric to analog, and the restoring forces sent to the host computer from analog to numeric, as described in Figure 5.

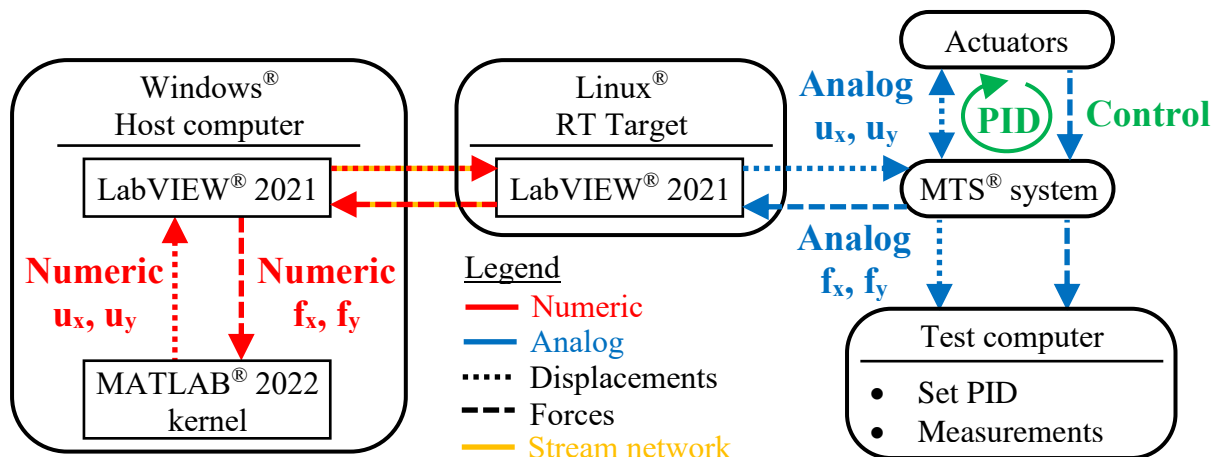


Figure 5: Data exchanges between the components of the experimental set-up.

The host computer and the RT target communicated in real time through a lossless stream network sending data to a LabVIEW[®] 2021 interface. The finite element analysis was performed on a

MATLAB[®] 2022 kernel running simultaneously on the host computer. The Benchmark comparison in Section 5.2 proved that this approach is by far the most efficient in the present case study.

5. Applications

5.1. CPU time-savings using a HROM

The POD and UDEIM modal bases were built using a set of 1680 displacement and force snapshots selected every 10 ms according to the sampling period of the ground motion. All the snapshots (i.e., training data) were computed using the results of an offline dynamic analysis performed on the full structure under hybrid test conditions. An implicit Newmark method was used with a Newton-Raphson algorithm for this purpose, while the α -OS method was applied during the HiL RT hybrid test.

A sensitivity analysis was first performed to find the lowest value of the number n of POD modes guaranteeing a satisfactory accuracy of the result. When n was set, a second sensitivity analysis was then carried out to define the number of elements in the RID. All calculations were performed on the host computer described in Section 4.2 using custom procedures implemented in MATLAB[®] software. The reduced solutions are compared to the FOM in Figure 6 using a strain energy error.

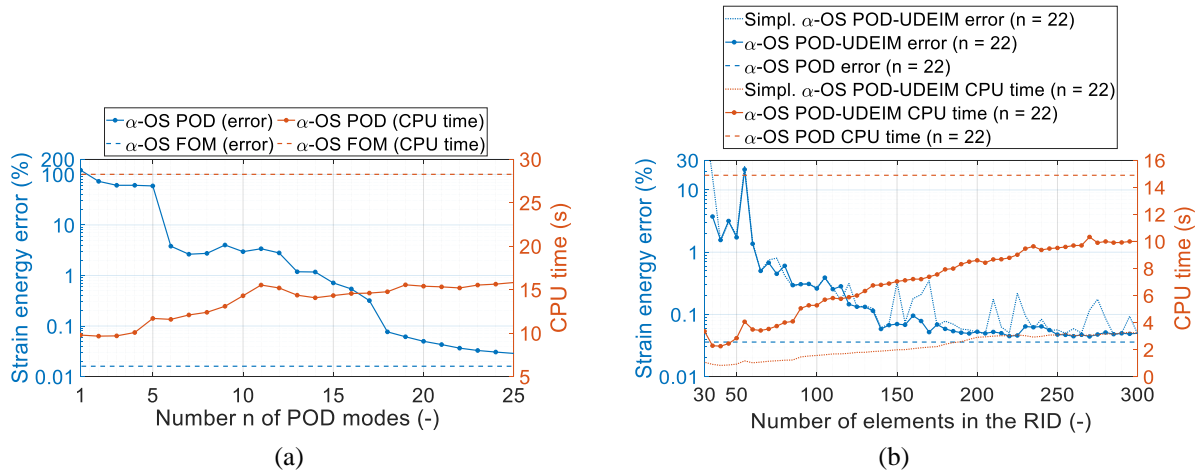


Figure 6: Error and online CPU time versus: the number of POD modes (POD) (a), and the number of elements in the RID with 22 POD modes (POD-UDEIM) (b).

Figure 6 (a) shows that the error does not exceed 0.04 % using the 22 POD modes defined by the highest singular values. Figure 6 (b) then proves that the online CPU time can be further reduced using a UDEIM procedure with a RID including 140 elements (~ 32 % of the mesh, see Figure 7 (a)).

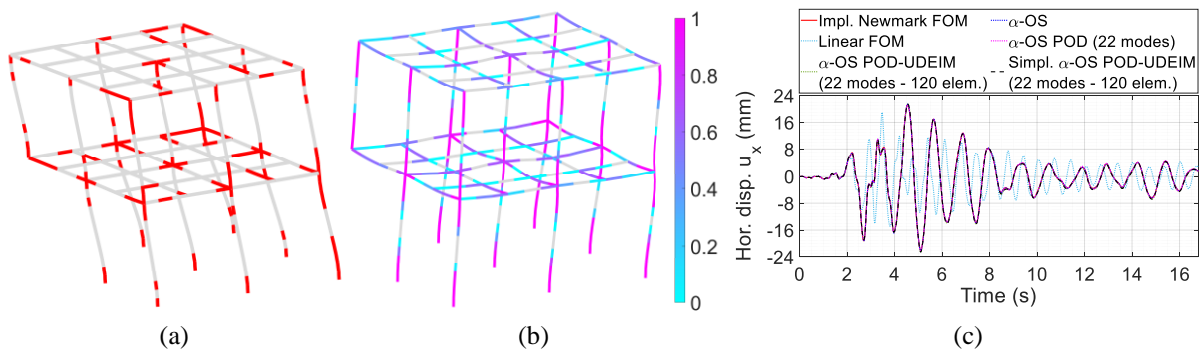


Figure 7: First POD mode and RID made of 140 beam elements (see the red lines) (a), final damage index on the FOM (354 damaged elements) (b), and horizontal displacement of the common node along the x -axis (c).

The resulting online phase lasts 6.67 s and proceeds accurately in less than 4 ms per time step (i.e., above the real time). Further simplifications (e.g., increasing the local strain increments of the concrete material law from 10^{-5} m/m to 10^{-4} m/m, or not updating the steel fibers properties since they remain elastic in the present case study) makes it possible to reach the same accuracy with an online phase lasting 2.01 s (i.e., approximately 1.2 ms per time step, see the orange dotted curve in Figure 6 (b)). The horizontal displacement of the common node (see Figure 2 (a)) plotted in Figure 7 (c) along the x -axis shows that the simplified POD-UDEIM HROM agrees well with the FOM despite the appearance of material nonlinearities on 354 damaged elements (see the colored lines in Figure 7 (b)).

Even if the delay of the analysis is lower than the sampling period, the efficiency of the HiL procedure still highly depends on the method used to implement the finite element functions in LabVIEW® (e.g., shared library, NET assembly, MATLAB calls, or scripts). A Benchmark comparison is performed in Section 5.2 to find the best method to use for RT hybrid testing.

5.2. Method used to implement the finite element functions in the HiL procedure

The finite element functions need to be directly called from the acquisition software during HiL hybrid tests. Several approaches are available in LabVIEW®, but their efficiency is still an open question in the case of RT hybrid tests involving high dimensional nonlinear models. LabVIEW® proposes to either use an interpreted MATLAB® script (i.e., MathScript®), a kernel running MATLAB® functions, compiled C shared libraries, or .NET assemblies. In this section, all these methods are compared on the Benchmark case study presented in Section 4.1. The finite element functions were deployed on the Windows® host computer and the RT target when the device compatibility allowed it (e.g., Shared libraries, or MathScript®). The analysis was carried out from 0 to 30 s with a time step of 10 ms. The delay due to the solving process is plot versus time in Figure 8, while the average delays are summarized in Table 1.

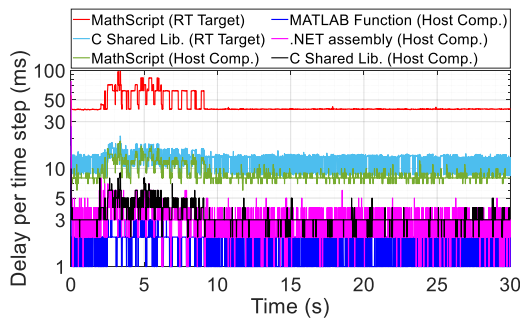


Figure 8: Delay per time step.


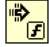
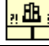

Method	Symbol	Average delay (ms)	
		Host computer	RT Target
MathScript®		8.9	44.6
Call MATLAB® functions		1.5	-
C shared library		3.3	12.4
.NET assembly		2.6	-

Table 1: Average delay related to each tested method.

Calling MATLAB® functions in the Windows® host computer is by far the most efficient method with average and maximum delays equal to 1.5 and 3.0 ms, respectively. The vectors and the matrices remain in the MATLAB® kernel as persistent variables so that few data are exchanged with LabVIEW®. As 7 to 9 ms can be saved for the actuators, MATLAB® function calls were thus used to perform the RT hybrid test presented in Section 4.

5.3. Experimental results

The RT hybrid test was performed from 0 to 30 s, with commands updated in the Windows® host computer and sent to the actuators every 10 ms using the Linux® RT target. The data acquisition was ensured by the MTS® system with a sampling frequency of 2^{10} Hz (i.e., every 0.97 ms). The commands and the horizontal displacements of the actuators are plotted in Figure 9 (a) and (b) along the x and y -axes, respectively. The results show that the measurements (blue curves) perfectly agreed with the command (red curves) for both actuators. The displacement along the x -axis was also in accordance with its theoretical value, even if slight variations appeared after the strong motion phase of the earthquake. This statement is not true along the y -axis since the amplitude of the displacement was lower

than the expected value. This could be due to nonlinearities introduced in the steel assemblies (e.g., gaps, contacts, or friction), excessive deformations of the steel frame (see Figure 4 (a)), or interactions between the actuators when the hybrid test proceeded. The latter could also explain why the force component measured along the x -axis was in better agreement with its theoretical value in compression than in tension (see Figure 10 (a)).

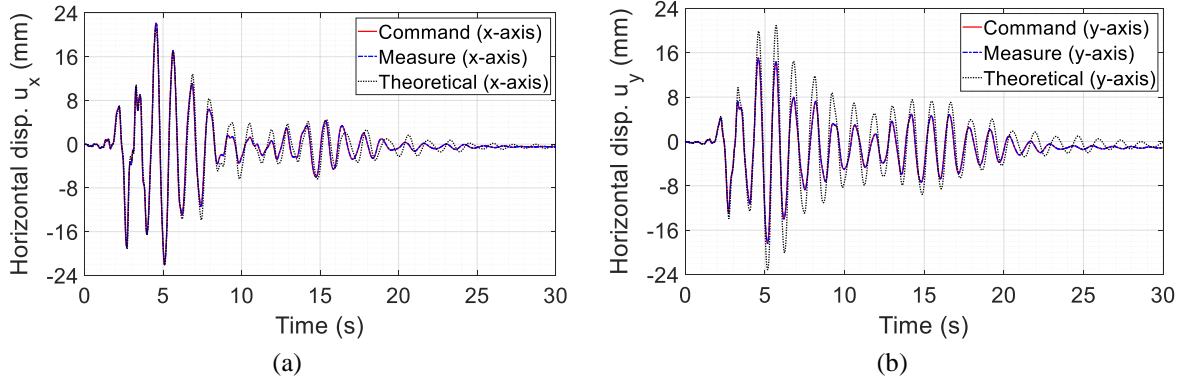


Figure 9: Commands, experimental, and theoretical values of the displacements applied by the actuators at the top of the steel column: x -axis (a), and y -axis (b).

The noise of the force sensors may also have led to errors as its amplitude exceeded 1.5 kN during the strong motion phase (see Figure 10 (a) at time 5 s), which is significant since the expected value was less than 12 kN. Further investigations are required to reduce the uncertainties due to interactions between the components of the experimental set-up and measurement errors. Despite these testing issues, the HiL procedure was thus able to successfully run the nonlinear FEM analysis and control the actuators in real time since the delay of the overall process remained above the sampling period of the ground motion (i.e., 10 ms) with a value from 7 ms to 9 ms (see Figure 10 (b)).

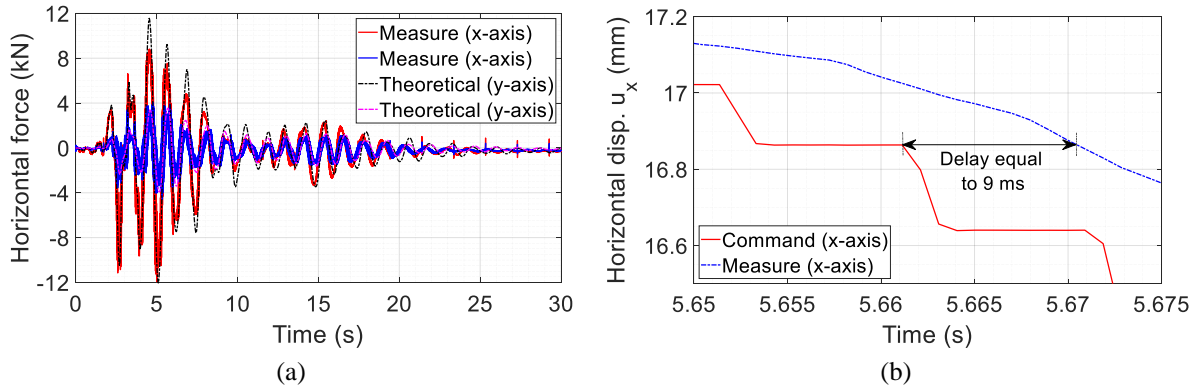


Figure 10: Experimental and theoretical values of the restoring forces (a), and delay of the HiL procedure by comparison between the command and the measure along the x -axis (b).

6. Conclusions

This paper presented a bidirectional real time hybrid test on a steel column virtually connected to a two-story reinforced concrete structure under earthquake conditions. The numerical substructure was meshed using Timoshenko multi-fiber beam elements. Nonlinearities were introduced from damage and elastic-plastic laws modeling the concrete and the steel fibers, respectively. A POD-UDEIM hyper reduced order modeling method first decreased the computational cost of the nonlinear model. The high dimensional system, initially made of 2382 free DOFs, was reduced on a basis of 22 POD modes, while the restoring force vector was approximated using a RID made of 140 elements (i.e., 32 % of the mesh).

Further simplifications (e.g., increasing the local strain increments in the concrete material law, or not updating the properties of the steel fibers) made it possible to accurately run the dynamic analysis with a delay approximately equal to 1.2 ms per time step, which is far above the sampling period of the ground motion (i.e., 10 ms). A Benchmark comparison of the methods available in Labview® for running the FEM analysis (e.g., MathScript® module, C Shared Libraries, or .NET assemblies) then showed that calling a MATLAB® kernel running on the Windows® host computer is the best strategy since the delay due to the dynamic analysis does not exceeded 3.0 ms in the present case study. A Linux® RT target exchanging data with the host computer through a lossless stream network was next used to perform a hybrid test. The overall procedure saved enough time to allow the dynamic actuators for accurately reaching their command in real time, despite using a simulated substructure modeled by a costly nonlinear numerical model. Improvement of the experimental set-up to reduce uncertainties and test a reinforced concrete column are currently under study.

References

- [1] Buchet, P., & Pegon, P. PsD testing with substructuring: Implementation and use. *Special publication, ISPRA*, I.94.25, 1994.
- [2] Nakashima, M., Kato, H., & Takaoka, E. Development of real-time pseudo dynamic testing. *Earthquake Engineering and Structural Dynamics*, 21(1):79-92, 1992.
- [3] Pegon, P., & Pinto, V. Pseudo-dynamic testing with substructuring at the ELSA Laboratory. *Earthquake Engineering and Structural Dynamics*, 29:905-925, 2000.
- [4] Nguyen, T. Analyses du comportement de rupteurs thermiques sous sollicitations sismiques. *PhD Thesis, ENS Cachan (In French)*, 2012.
- [5] Souid, A., Delaplace, A., Ragueneau, F., & Desmorat, R. Pseudo-dynamic testing and nonlinear substructuring of damaging structures under earthquake loading. *Engineering Structures*, 31(5):1102-1110, 2009.
- [6] Lebon, G. Analyse de l'endommagement des structures de Génie Civil : techniques de sous-structuration hybride couplées à un modèle d'endommagement anisotrope. *PhD Thesis, ENS Cachan (In French)*, 2011.
- [7] Moutoussamy, L. Essais hybrides en temps réels sur structures de Génie Civil. *PhD Thesis. ENS Cachan (In French)*, 2013.
- [8] Ayoub N., Deü J.-F., Larbi W., Pais J., Rouleau L. (2022). Application of the POD method to nonlinear dynamic analysis of reinforced concrete frame structures subjected to earthquakes, *Engineering Structures*, 270, 114854 (9 pages).
- [9] Tiso P., Rixen D. J. Discrete empirical interpolation method for finite element structural dynamics. *Nonlinear Modelling and Applications, Volume 2. Springer*, 53-65, 2013.
- [10] Hilber, H., Hugues, T., & Taylor, R. Improved numerical dissipation for time integration algorithms in structural dynamics. *Earthquake Engineering and Structural Dynamics* 5(3), 282-292, 1977.
- [11] Bodnar B., Larbi W., Titirla M., Deü J.-F., Gatuingt F., Ragueneau F. Modelling of a PsD hybrid test on a RC column/beam junction combining a multifibre beam model and a POD-ROM approach. *Computational Modelling of Concrete Structures, Euro-C 2022*, May 2022, Vienne, Austria. 414 - 423, 2022.
- [12] Combescure D., Pegon P., Magonette, G. Numerical investigation of the impact of experimental errors on various pseudo-dynamic integration algorithms. *Proceedings of the 10th European Conference on Earthquake Engineering, Duma G. (ed.). Balkema, Rotterdam, The Netherlands*, 2479-2484, 1995.
- [13] Davenne L., Ragueneau F., Mazars J., Ibrahimbegovic A. Efficient approaches to finite element analysis in earthquake engineering. *Computers and Structures* 81, 1223-1239, 2003.
- [14] Richard B., Ragueneau F. Continuum damage mechanics based model for quasi brittle materials subjected to cyclic loadings: Formulations, numerical implementation and applications. *Engineering Fracture Mechanics* 98, 383-406, 2013.